RESEARCH ARTICLE

Empirical Model Of Unreinforced Beam-column RC Joints With Plain Bars

Teresa De Risi Maria[*], Ricci Paolo and Verderame Gerardo Mario

Department of Structures for Engineering and Architecture, University of Naples Federico II, Naples, Italy

Abstract:

Background:

Nonlinear behaviour of beam-column joints might significantly affect seismic performance of typical existing buildings, especially in the case of poor structural detailing, as the lack of an adequate transverse reinforcement in the joint panel or deficiencies in the anchorage details. A very limited number of studies deals with beam-column joints reinforced with plain hook-ended longitudinal bars, widespread in Mediterranean building stock, or with the analysis of local aspects, such as the evaluation of joint shear strain capacity. The almost totality of the models proposed in the literature for simulating the cyclic behaviour of RC joints was calibrated by means of tests performed on elements with deformed bars. Such models may be not suitable for elements with hook-ended plain bars, due to their peculiarities in terms of failure mode and concrete-to-steel interaction mechanisms.

Objective:

An empirical macro-modeling approach is proposed in this work for exterior unreinforced joints with hook-ended plain bars, suitable for extensive nonlinear analyses.

Methods:

A dedicated database of experimental tests is first collected. Based on this dataset, a shear strength model is developed. The joint panel constitutive parameters are also defined to reproduce the cyclic experimental joint shear stress-strain behaviour.

Results:

The whole modeling approach is validated through the comparison with the collected experimental data. It well reproduces the global response, in terms of elastic stiffness, global deformability, softening stiffness, unloading and reloading stiffness degradation and pinching effect for all the investigated tests.

Conclusion:

The proposed model thus results reliable for the investigated typology of beam-column joints.

Keywords: Reinforced concrete buildings, Exterior unreinforced joints, Plain bars, Empirical model, Shear strength, Hysteretic behaviour.

1. INTRODUCTION

Past and more recent earthquakes in the Italian and Mediterranean area have shown a high vulnerability of the existing building stock subjected to ground shaking [1 - 3]. The overwhelming majority of the existing Reinforced Concrete (RC) buildings is "non-conforming" to the most recent and updated technical and seismic codes. The design of such buildings was often proposed only for gravity loads or according to old seismic codes. In these cases, no

* Address correspondence to this author at the Department of Structures for Engineering and Architecture, University of Naples Federico II, *via* Claudio, 21 - 80125, Naples, Italy; Tel: +39 0817683341; Email:mariateresa.derisi@unina.it

strength hierarchy principles have been applied by the designers, so that, generally, shear failures are very likely, especially in beam-column intersections without a proper transverse reinforcement, thus limiting the achievement of the flexural capacity of the ductile elements [4, 5].

In the last decades, a significant amount of experimental studies has been performed to assess the seismic performance of unreinforced beam-column intersections (*e.g.*, [6 - 8]). These studies often analyzed the beneficial or detrimental effect of some parameters (for example column axial load, concrete strength, joint aspect ratio, or beam longitudinal reinforcement ratio) on joint shear strength. Few researchers try to experimentally assess the seismic performance of joints without stirrups in the joint core and with plain hook-ended longitudinal reinforcing bars in beams and columns, widespread in the existing RC building stock of the Mediterranean region. Some of them tested beam-column joints with a minimum amount of transverse reinforcement in the joint panel [9 - 11], or assessed the effect of axial load ratio [9, 11] or different anchorage details [9, 11, 12] on joint shear strength and hysteretic dissipation capacity. Other works in the literature also compared the experimental performance of interior and exterior joints with plain bars without stirrups in the joint core [13 - 15] or tested possible retrofitting strategies mainly to increase the shear strength of this joint typology (*e.g* [16].). These experimental studies proved that exterior joints are more vulnerable to shear failures with respect to interior joints [15] and highlighted *(i)* the influence of the slippage of longitudinal bars on the response of such elements [15, 17], and *(ii)* a typical failure mode that exhibits the detachment of a concrete wedge from column cover especially for exterior joints (mainly due to the stress concentration at the hook anchorage location after the shear cracking of the joint panel) [13]. Finally, eight tests were performed by the authors [18 - 21] on unreinforced exterior beam-column joints, comparing the performance of joints with plain and deformed bars, and investigating about the effect of beam longitudinal reinforcement amount and joint aspect ratio on joint shear strength, failure mode, and deformability contributions.

The number of tests performed on RC joints without a proper transverse reinforcement with hook-ended plain bars in beams and columns is certainly very low if compared with the amount of data available for unreinforced RC joints with deformed bars [19]. Furthermore, these few tests are generally designed and realized to reproduce different constructive practices, typical of different countries, resulting in a great inhomogeneity in terms of main features of the specimens (*e.g.* anchorage details, or presence of a minimum amount of ties in the joint core). Researchers often focused their attention mainly on the joint shear strength; thus, only a few of them provided experimental values for joint shear strains, nevertheless the crucial role of these data to reproduce the seismic behaviour of joints through numerical modelling in a reliable way.

Furthermore, only two strength models exist in literature properly for this joint typology. The first one was proposed by Pampanin *et al*. [13]. On the basis of two tests on T-joints, they proposed a limitation of the traditional shear strength model adopted for joints with deformed bars [22], which appeared to be necessary due to the peculiarities of the observed failure mode (with the above-mentioned detachment of a concrete cover wedge). The resulting joint shear strength only depends on concrete compressive strength, not taking into account the effects of other parameters such as joint aspect ratio or longitudinal reinforcement of the adjacent members (often defined as key parameters, for example, by Park and Mosalam [23] for joints with deformed bars). The second model was more recently proposed by Metelli *et al*. [24], on the basis of a modification of the mechanical-based approach by Hwang and Lee [25] and a validation phase based on five tests with plain bars.

Certainly, more experimental data are necessary to assess and validate the existing models or to propose a new model for this kind of elements due to their peculiarities in failure mode and steel-concrete interaction quality. Furthermore, a complete characterization of the nonlinear local response of the joint panel and fixed-end-rotation contribution is necessary to clearly understand the joint behavior under cyclic loading and to reliably model this element for structural analyses of non-conforming RC frames. Therefore, in this work, an empirical macro-modeling approach is proposed for exterior unreinforced joints with hook-ended plain bars in beam and columns, suitable for extensive nonlinear analyses. A dedicated database of experimental tests is first collected. Based on this dataset, a proper shear strength model is carried out, starting from the analysis of previous proposals from the literature. The joint panel constitutive parameters are also defined to reproduce the cyclic experimental joint shear stress-strain behaviour. Finally, the whole modeling approach is validated through the comparison with experimental results.

2. EXPERIMENTAL DATABASE

Data about tests on exterior unreinforced RC joints with plain hook-ended longitudinal bars are first collected from the literature. In the literature, there are a very small number of tests about this structural typology. Some of them

reproduce the presence of the RC slab or of the transverse beam (*e.g* [26].); some others also consider the presence of welded (not hook-ended) longitudinal bars of the beam [11]. Nevertheless, in this study, a homogeneous subset of tests has been analyzed, namely only tests without transversal beams or slab and hook-ended bars are considered; therefore, 16 tests belong to the presented database, on the whole. Main geometrical and mechanical properties of these specimens are reported in Table **1**.

Table 1. Database of collected experimental tests.

#	Reference	ID	ν	b_c	h_c	b_b	h_b	f_c	$A_{s,b,bot}$	$A_{s,b\,top}$	$A_{s,c}$	L_b	L_c
	(-)		(mm)	(mm)	(mm)	(mm)	(mm)	(MPa)	(mm²)	(mm²)	(mm²)	(mm)	(mm)
1	Genesio	pre1970s	0.21[(+)]	230	230	230	330	17.7	314	314	236	1409	835
2	[33]	JT2-1	0.00	350	300	300	400	24.4	829	829	943	1700	1415
3	Bedirhanoglu *et al.* [11]	JO5	0.13	250	500	250	500	8.3	804	804	804	1360	1250
4	Pampanin *et al.* [13] and Moratti	T1	0.13[(+)]	200	200	200	330	23.9	327	327	151	1500	1000
5	[42]	T2	0.13[(+)]	200	200	200	330	23.9	214	214	151	1500	1000
6		TPA-1	0.13	250	250	250	400	24.2	339	339	226	1875	1300
7		TPA-2	0.12	250	250	250	400	25.8	339	339	226	1875	1300
8	Melo *et al.* [12]	TPB-1	0.20	250	250	250	400	15.8	339	339	226	1875	1300
9		TPB-2	0.12	250	250	250	400	27.3	339	339	226	1875	1300
10		TPC	0.13	250	250	250	400	23.8	339	339	226	1875	1300
11	Ricci *et al.* [19]	1P	0.10	300	300	300	500	28.7	1257	1257	1257	1650	1450
12		2P	0.10	300	300	300	500	28.7	616	616	616	1650	1450
13		1bP	0.10	300	300	300	400	17.7	1257	1257	1257	1650	1500
14	De Risi and Verderame [20]	2bP	0.10	300	300	300	400	17.7	804	804	1257	1650	1500
15		1cP	0.10	300	300	300	600	17.7	1257	1257	1257	1650	1400
16		2cP	0.10	300	300	300	600	17.7	804	804	1257	1650	1400

(*) corresponding to the maximum achieved beam/column shear

All of these tests were (i) characterized by low-medium concrete compressive strength (f_c) and weak beam-strong column hierarchy and (ii) generally performed by applying a constant axial load (N) on the column (except than for tests #1, 4, 5), and an imposed displacement history on the beam (loading scheme (LS) "beam") or column (LS "column") tip. In Table **1**, L_b and L_c represent the beam and column clear length, respectively. The parameters b_b and b_c are the beam and column width, respectively; h_b and h_c are the beam and column height, respectively. $A_{s,b,bot}$, $A_{s,b,top}$ are bottom and top longitudinal reinforcement in beam; $A_{s,c}$ represents longitudinal reinforcement in the column. Finally, ν is the column axial load ratio ($\nu = N/(b_c \cdot h_c \cdot f_c)$).

For each collected test, Table **2** shows the maximum beam shear measured during the test ($V_{b,TEST}$), the shear corresponding to beam yielding ($V_{b,yield}$) and the "observed" failure mode (FM) - namely, joint failure after beam yielding, BJ-mode, or without beam yielding, J-mode - which can be determined by comparing these two values. The shear corresponding to the flexural strength of the beam ($V_{b,flex}$) - evaluated only for BJ-failure modes - is also reported. In particular, the yielding moment and the flexural strength are evaluated on a fibre section by assuming Mander *et al.* [27] constitutive relationship for concrete and elastic-plastic with strain hardening relationship for reinforcing steel.

Table 2. Experimental joint shear strength, observed failure mode, yielding and flexural capacity.

Test	$V_{b,TEST}$ (*)	$V_{b,yield}$	$V_{b,flex}$	FM obs (**)	$\dfrac{\tau_{j,TEST}}{\sqrt{f_c}}$	$\dfrac{\tau_{j,yield}}{\sqrt{f_c}}$	$\dfrac{\tau_{j,flex}}{\sqrt{f_c}}$	Experimental Joint Shear Strain
#	(kN)	(kN)	(kN)		(MPa^{0.5})			
1	24.80	26.82	-	J	0.49	0.53	-	no
2	41.50	47.89	-	J	0.44	0.50	-	no
3	51.50	82.86	-	J	0.39	0.63	-	no
4	16.00	22.91	-	J	0.38	0.55	-	no
5	16.10	15.16	18.87	BJ	0.39	0.36	0.45	no
6	28.20	25.26	31.57	BJ	0.44	0.39	0.49	no

Test	$V_{b,TEST}$ (*)	$V_{b,yield}$	$V_{b,flex}$	FM obs (**)	$\dfrac{\tau_{j,TEST}}{\sqrt{f_c}}$	$\dfrac{\tau_{j,yield}}{\sqrt{f_c}}$	$\dfrac{\tau_{j,flex}}{\sqrt{f_c}}$	Experimental Joint Shear Strain
#	(kN)	(kN)	(kN)		(MPa$^{0.5}$)			
7	29.40	25.29	31.60	BJ	0.44	0.38	0.47	no
8	27.75	24.97	31.47	BJ	0.53	0.48	0.60	no
9	29.55	25.35	31.56	BJ	0.43	0.37	0.46	no
10	27.30	25.25	31.59	BJ	0.42	0.39	0.49	no
11	79.24	109.38	-	J	0.57	0.78	-	yes
12	52.82	50.59	77.94	BJ	0.38	0.36	0.55	yes
13	51.70	89.58	-	J	0.62	1.41	-	yes
14	50.30	52.50	-	J	0.60	0.80	-	yes
15	68.40	165.50	-	J	0.50	1.47	-	yes
16	46.90	83.56	-	J	0.34	0.82	-	yes

(*) $V_{b,TEST}$ is the maximum experimental beam shear. When LS is "column", $V_{b,TEST}$ is obtained from the rotational equilibrium of the (iso-static) sub-assemblage

(**) FM obs. = observed failure mode: "J"=joint shear failure without beam yielding; "BJ"=joint shear failure after beam yielding.

Joint shear (V_{jh}) is obtained from beam shear (V_b) through equilibrium equations, based on the geometrical characteristics of the specimens, by using Eq. (1):

$$V_{jh} = T\text{-}V_c = \frac{V_b \cdot L_b}{d^*} - \frac{V_b \cdot (L_b + h_c/2)}{(2L_c + h_b)} = V_b \cdot L_b \left[\frac{1}{d^*} - \frac{1 + h_c/(2L_b)}{(2L_c + h_b)} \right] \tag{1}$$

where d^* is the internal lever arm of the beam, defined as $d^* \cdot d$, and d is the effective depth. Fiber section analyses provide, on average, k=0.90 at beam yielding [19]. Hence, the shear stress values corresponding to peak strength ($\tau_{j,TEST}/\sqrt{f_c}$), beam yielding ($\tau_{j,yield}/\sqrt{f_c}$) and beam flexural strength ($\tau_{j,flex}/\sqrt{f_c}$) can be calculated by dividing the corresponding joint shear V_{jh} by the horizontal joint area, A_{jh} (Table **2**).

It is worth noting that $\tau_{j,TEST}/\sqrt{f_c}$ results to increase if mechanical reinforcing percentage in the beam (ω_b) increases, whereas $\tau_{j,TEST}/\sqrt{f_c}$ decreases when joint aspect ratio (h_b/h_c) increases (Fig. **1**), as also observed in [19, 20].
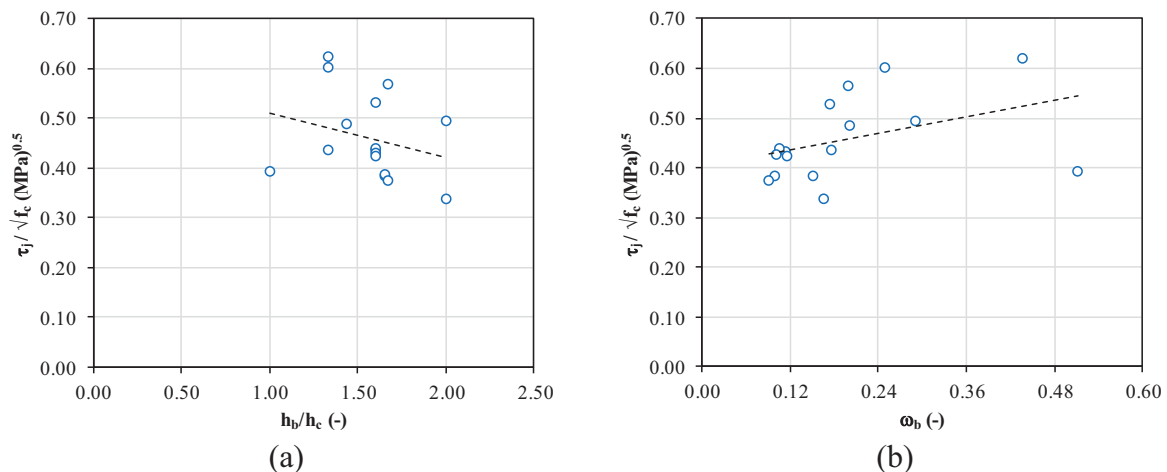

Fig. (1). Experimental trends of joint shear strength depending on joint aspect ratio **(a)** and beam mechanical reinforcing percentage **(b)**.

Furthermore, note that in only six cases (*i.e.*, tests by [19, 20]), joint shear strain evolutions under cyclic loading are experimentally obtained and explicitly presented by the Authors (see the last column in Table **2**).

3. SHEAR STRENGTH MODEL

Experimental peak shear strength for the collected tests is compared with the prediction of some of the main capacity models from literature and codes for unreinforced beam-column exterior joints, thus evaluating their

effectiveness, also depending on the observed failure mode. Four of the most consolidated existing capacity models, namely models by Priestley [28], ASCE-SEI 41 [29], Park and Mosalam [23] and Jeon *et al*. [30], are analysed in Section 3.1, together with the model proposed by Pampanin *et al*. [13], which is specifically obtained from tests related to joints with hook-ended plain bars, as explained in Section 1. Then a new empirical model is proposed and presented in Section 3.2 to improve the accuracy of the predicted shear strength for the investigated joint typology.

3.1. Models From Literature

The experimental values of maximum joint shear stress ($\tau_{j,max}/\sqrt{f_c}$) are compared with shear strength predictions by some of the main and most recent predictions from literature.

One of the mainly adopted shear strength models for unreinforced joints in literature was proposed by Priestley [28]. Such a proposal limits the maximum allowable value of the principal tensile stress to $0.42\sqrt{f_c}$, so that joint shear strength can be computed as shown in Eq. (2):

$$\tau_{j,max}\Big/\sqrt{f_c} = 0.42\sqrt{1 + \frac{N}{0.42\sqrt{f_c}\,A_{jh}}} \qquad (2)$$

More recently, also Park and Mosalam [23] proposed a mechanical approach for exterior unreinforced joints. According to this model, joint shear strength decreases if beam yielding occurs due to the detrimental effect on the bond quality between concrete and steel after yielding. In this case, joint shear strength can be obtained from Eq. (3):

$$\tau_{j,max}\Big/\sqrt{f_c} = k\left[\frac{\cos\theta}{\cos(\pi/4)}\right] \qquad \text{with } \theta = \arctan\left(\frac{h_b}{h_c}\right) \qquad (3)$$

In Eq. (3), $\tau_{j,max}$ depends on the joint aspect ratio (h_b/h_c) and the coefficient *k* accounts for the effect of the beam longitudinal reinforcement ratio (it also provides a failure mode prediction [23]).

A regression-based shear strength model has been also proposed by Jeon *et al*. [30] on the basis of a huge amount of collected experimental data on beam-column joints. Jeon *et al*. [30] proposed a probabilistic model for unreinforced exterior joints assuming that joint shear strength depends on (Eq. 4): concrete compressive strength (f_c), maximum joint shear demand (τ_d), in-plane and out-of-plane geometry factors JP (assumed equal to 0.75 for exterior joints, respectively) and TB (equal to 0 if less than two transverse beams are present), joint aspect ratio, column-to-beam nominal moment strength ratio (M_R), and ratio of intermediate column reinforcement strength to design joint shear demand (β).

$$\ln(\tau_{j,max}) = -0.81 + 0.46\ln(f_c) + 0.50\ln(\tau_d) + 0.68\ln(JP) + 0.62\ln(TB) + $$
$$-0.25\ln(h_b/h_c) + 0.08\ln(M_R) + 0.14\ln(\beta) \qquad (4)$$

For all the above-mentioned models, the totality of experimental data adopted for the calibration or the validation of the proposals was related to joints with deformed longitudinal reinforcing bars.

Vice-versa, specifically for exterior joints with hook-ended plain longitudinal rebars and without transverse reinforcement in the joint core, only Pampanin *et al*. [13] and Metelli *et al*. [24] carried out two proposals for joint shear strength, even if (necessarily) calibrated-on/compared with a very small number of experimental tests from literature. In particular, Pampanin *et al*. [13] suggest to modify the proposal by Priestley [22] by limiting the principal tensile stress (p_t) at the first joint cracking, namely at $0.20\sqrt{f_c}$. Therefore, according to this joint strength model, peak strength is assumed to be equal to the cracking strength, as shown in Eq. (5):

$$\tau_{j,max}\Big/\sqrt{f_c} = 0.20\sqrt{1 + \frac{N}{0.20\sqrt{f_c}\,A_{jh}}} \qquad (5)$$

Metelli *et al*. [24] also adopted the latter model and concluded that the mean relative error evaluated on some experimental tests from literature is, on average, the closest to zero.

The results of the comparisons between experimental shear strength and predicted values according to the above-mentioned models are reported in Table **3** and graphically shown in Fig. (**2**).
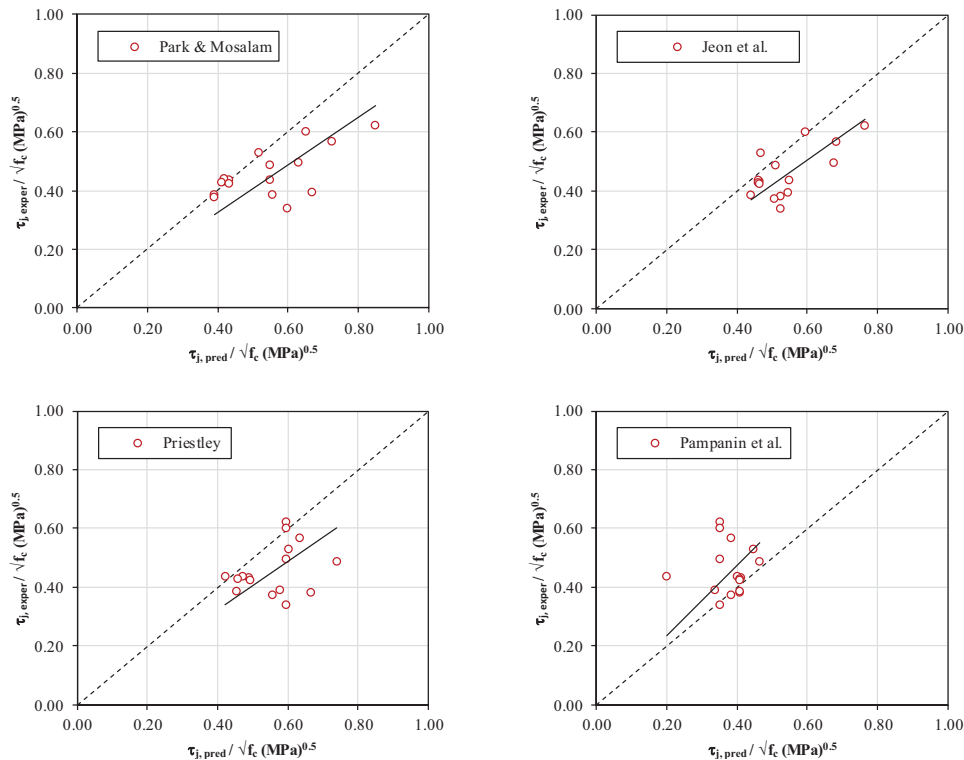

Fig. (2). Experimental ("exper") versus predicted ("pred") joint shear strength for the investigated models from literature (solid black lines represent the linear regression trends).

For each one of the capacity models mentioned above the predicted shear strength ($\tau_{j,pred}/\sqrt{f_c}$) is calculated for all tests. It is worth noting that, since the joint shear demand cannot exceed the joint shear compatible with beam flexural capacity (in cases of weak beam/strong column), $\tau_{j,pred}/\sqrt{f_c}$ should be limited to $\tau_{j,flex}/\sqrt{f_c}$. This limitation is already implicit for models by Park and Mosalam [23] and Jeon *et al*. [30], since their definition of joint shear strength. When $\tau_{j,pred}/\sqrt{f_c}$ has been limited to $\tau_{j,flex}/\sqrt{f_c}$ the predicted-to-experimental ratio is highlighted in grey in Table **3**.

Generally speaking, joint shear strength capacity models proposed for unreinforced joints with deformed longitudinal reinforcement, like [23] and [30], overestimate the shear strength of joints with plain bars (by 20% and 19%, respectively). Such an overestimation is observed, in particular, in the case of J-failure mode (+37% and +27% respectively, for models by [23] and [30], respectively), and less significantly in the case of BJ-failure mode (-1% and +10%, respectively). This result, according to the approach of Park and Mosalam [23], can be likely explained by the higher strength contribution developed by the bond resistance of the concrete surrounding the beam reinforcement in joints with deformed longitudinal reinforcement, compared to joints with plain longitudinal reinforcement [19].

Similarly, also the model by Priestley [28] overestimates the shear strength of joints with plain bars, by 24%; again, such an overestimation is higher in the case of J-failure mode (+30%) and lower in the case of BJ-failure mode (+17%). In the case of observed BJ-mode, it has to be noted that, for Priestley's [28] model, the predicted shear strength has to be limited to the beam flexural strength in all cases. In these cases, the predicted-to-experimental ratio does not depend on the joint shear strength predicted by the model, but rather on the predicted beam flexural strength; thus, the predicted-to-experimental ratio does not represent the predictive capacity of the model. On the contrary, the model by Pampanin *et al*. [13], proposed as a modification of the model by Priestley [28] for joints with plain bars, underestimates the joint shear strength on average by 15%, showing, in particular, a good predictive capacity in the case of BJ-failure mode.

3.2. Proposed model

In the previous Section, it has been observed that main shear strength models proposed in the literature for unreinforced beam-column joints with deformed bars overestimate, on average, the experimental joint shear strength. Such an overestimation is likely due to the overestimation of the strength contribution developed by the bond resistance of the concrete surrounding the beam reinforcement, compared to joints with plain longitudinal reinforcement, as already observed in [19]. On the contrary, the lonely model proposed for unreinforced joints with hook-ended plain bars underestimates the experimental strength. Joint shear strength predicted by such a model does not depend on joint aspect ratio or beam longitudinal reinforcement, thus resulting in not being able to reproduce the experimental trends found and presented in Fig. (**1**). Therefore, a new simple shear model, empirically-based, is proposed herein starting from the analysis of the tests results from the collected database.

First of all, it has been already observed that joint shear strength decreases when the joint aspect ratio decreases. This behavior can be ascribable to a compressive-strut mechanism developing in the unreinforced joint core, which is able to provide a higher horizontal shear strength when its inclination with respect to the horizontal direction (Θ) decreases [23, 28]. If tests characterized by a J-failure mode are first analyzed, such a trend can be described by means of the red regression curve reported in Fig. (**3a**). A similar trend has been found for joints with deformed bars by Park and Mosalam [23], which finally proposed a relationship between joint aspect ratio and joint shear strength where the proportionality factor k (see Eq. 4) is assumed equal to the unity (instead than 0.6, as proposed herein for joints with plain bars, based on the experimental evidence). Furthermore, it was observed that when the mechanical longitudinal reinforcement ratio of the beam decreases, joint shear strength also decreases (Fig. **1b**), in particular for the tests characterized by a BJ-failure mode, for which $\tau_{j,TEST}$ necessarily ranges between $\tau_{j,y}$ and $\tau_{j,flex}$. More in details, if tests with a BJ-failure mode are analysed, it can be observed that the joint shear strength can be assumed as proportional to $\tau_{j,y}$, in particular through a proportionality factor evaluated by means of the linear regression shown in Fig. (**3b**) and equal to 1.10, on average. Such a coefficient results higher than the unity likely due to a possible beam hardening that allows an increase in joint shear demand with respect to $\tau_{j,y}$ up to the achievement of joint shear strength.


(a) (b)
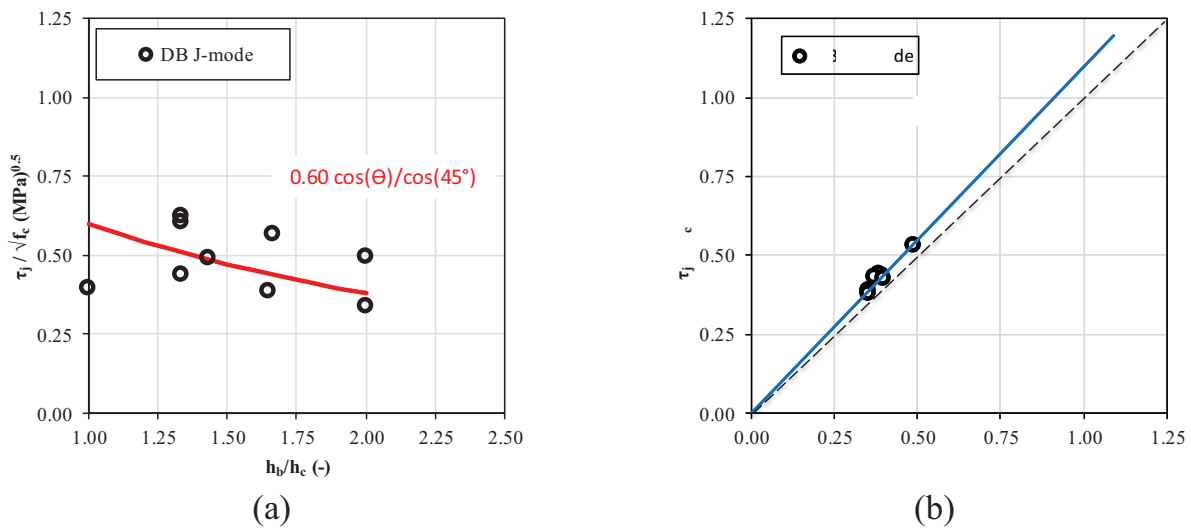
Fig. (3). Analysis of experimental trends from the collected database (DB) of joint shear strength depending on the aspect ratio for J-mode **(a)** and on joint shear demand at beam yielding for BJ-mode **(b)**.

In summary, joint shear strength can be predicted according to Eq. (6):

$$\tau_{j,max}/\sqrt{f_c} = \min\left(0.60 \cdot \frac{\cos\theta}{\cos 45°};\ 1.10 \cdot (\tau_{j,y}/\sqrt{f_c})\right) \tag{6}$$

Table 3. Joint shear predictions according to models from literature.

#	Obs FM	\multicolumn{3}{Experimental}			Priestley (1997)			Park and Mosalam (2012)			Jeon et al. (2014)			Pampanin et al. (2002)		
#	Obs FM	$\frac{\tau_{j,TEST}}{\sqrt{f_c}}$	$\frac{\tau_{j,yield}}{\sqrt{f_c}}$	$\frac{\tau_{j,flex}}{\sqrt{f_c}}$			$\frac{\tau_{j,pred}}{\sqrt{f_c}}$	pred FM	pred/ test	$\frac{\tau_{j,pred}}{\sqrt{f_c}}$	pred FM	pred/ test	$\frac{\tau_{j,pred}}{\sqrt{f_c}}$	pred FM	pred/ test	$\frac{\tau_{j,pred}}{\sqrt{f_c}}$	pred FM	pred/ test
		$(MPa)^{0.5}$	$(MPa)^{0.5}$	$(MPa)^{0.5}$			$(MPa)^{0.5}$			$(MPa)^{0.5}$			$(MPa)^{0.5}$			$(MPa)^{0.5}$		
1	J	0.49	0.53	-			0.74	BJ	1.52	0.55	BJ	1.13	0.51	J	1.05	0.47	J	0.96
2	J	0.44	0.50	-			0.42	J	0.96	0.55	BJ	1.26	0.55	BJ	1.26	0.20	J	0.46
3	J	0.39	0.63	-			0.58	J	1.47	0.67	BJ	1.70	0.54	J	1.39	0.34	J	0.86
4	J	0.38	0.55	-			0.67	BJ	1.75	0.56	BJ	1.45	0.52	J	1.36	0.41	J	1.06
5	BJ	0.39	0.36	0.45			0.45	BJ	1.17	0.39	BJ	1.01	0.44	BJ	1.14	0.41	BJ	1.06
6	BJ	0.44	0.39	0.49			0.49	BJ	1.12	0.43	BJ	0.99	0.46	BJ	1.07	0.41	BJ	0.94
7	BJ	0.44	0.38	0.47			0.47	BJ	1.07	0.42	BJ	0.96	0.46	BJ	1.05	0.40	BJ	0.92
8	BJ	0.53	0.48	0.60			0.60	BJ	1.13	0.52	BJ	0.97	0.47	J	0.89	0.45	J	0.84
9	BJ	0.43	0.37	0.46			0.46	BJ	1.07	0.41	BJ	0.96	0.46	BJ	1.08	0.41	BJ	0.95
10	BJ	0.42	0.39	0.49			0.49	BJ	1.16	0.43	BJ	1.02	0.46	BJ	1.09	0.41	BJ	0.96
11	J	0.57	0.78	-			0.63	J	1.12	0.73	J	1.28	0.69	J	1.21	0.38	J	0.68
12	BJ	0.38	0.36	0.55			0.55	BJ	1.48	0.39	BJ	1.04	0.51	BJ	1.35	0.38	BJ	1.02
13	J	0.62	1.41	-			0.59	J	0.95	0.85	J	1.36	0.77	J	1.23	0.35	J	0.57
14	J	0.60	0.80	-			0.59	J	0.99	0.65	BJ	1.08	0.60	J	0.99	0.35	J	0.59
15	J	0.50	1.47	-			0.59	J	1.20	0.63	J	1.28	0.68	J	1.37	0.35	J	0.71
16	J	0.34	0.82	-			0.59	J	1.76	0.60	BJ	1.77	0.53	J	1.55	0.35	J	1.04
\multicolumn{5}{ALL}				mean	1.24		mean	1.20		mean	1.19		mean	0.85
							CoV	0.21		CoV	0.22		CoV	0.15		CoV	0.23
\multicolumn{5}{J}				mean	1.30		mean	1.37		mean	1.27		mean	0.77
							CoV	0.25		CoV	0.17		CoV	0.14		CoV	0.29
\multicolumn{5}{BJ}				mean	1.17		mean	0.99		mean	1.10		mean	0.96
							CoV	0.12		CoV	0.03		CoV	0.13		CoV	0.07

The proposed empirical model described above is finally applied to all the collected tests presented in the previous section thus evaluating its accuracy (Table **4**). It can be noted that the mean predicted-to-experimental shear strength ratio is equal to 1.00 if all the tests are considered. Also, if only tests that exhibited a J-failure mode or a BJ-failure mode are considered separately, the mean relative error is very close to zero. As a matter of fact, a very slight underestimation is observed for BJ-mode tests (-3%) and a slight overestimation is obtained for tests with a J-failure mode (+2%). Coefficient of variation of such prediction results is quite limited (19%), especially for BJ-mode tests (7%), thus finally confirming a good accuracy of the proposed model.

Table. 4. Prediction errors related to the proposed empirical model.

#	Observed FM	$\frac{\tau_{j,TEST}}{\sqrt{f_c}}$	$\frac{\tau_{j,pred}}{\sqrt{f_c}}$	Pred FM	Pred/ test
		$(MPa)^{0.5}$	$(MPa)^{0.5}$		
1	J	0.49	0.51	J	1.00
2	J	0.44	0.55	J	1.17
3	J	0.39	0.54	J	1.53
4	J	0.38	0.52	J	1.14
5	BJ	0.39	0.44	BJ	1.03
6	BJ	0.44	0.46	BJ	0.99
7	BJ	0.44	0.46	BJ	0.95
8	BJ	0.53	0.47	J	0.85
9	BJ	0.43	0.46	BJ	0.95

(Table 4) contd.....

#	Observed FM	$\dfrac{\tau_{j,TEST}}{\sqrt{f_c}}$ $(MPa)^{0.5}$	$\dfrac{\tau_{j,pred}}{\sqrt{f_c}}$ $(MPa)^{0.5}$	Pred FM	Pred/ test
10	BJ	0.42	0.46	BJ	1.01
11	J	0.57	0.69	J	0.77
12	BJ	0.38	0.51	BJ	1.05
13	J	0.62	0.77	J	0.82
14	J	0.60	0.60	J	0.85
15	J	0.50	0.68	J	0.77
16	J	0.34	0.53	J	1.12
ALL				mean	**1.00**
				CoV	0.19
J				mean	**1.02**
				CoV	0.25
BJ				mean	**0.97**
				CoV	0.07

4. Stress-strain nonlinear behavior of the joint panel

Together with the joint shear strength assessment, a complete characterization of the nonlinear local response of the joint panel is certainly necessary to clearly understand the joint behavior under cyclic loading and to reliably model this element for structural analyses of non-conforming RC frames. Therefore, herein the shear behavior of the joint panel is empirically defined. In particular, the nonlinear shear stress (τ_j)-strain (γ_{joint}) response of the joint panel has been characterized by means of four characteristic points, as proposed by previous studies (*e.g* [4, 5, 31]): cracking, pre-peak, peak and residual points (Fig. **4**).
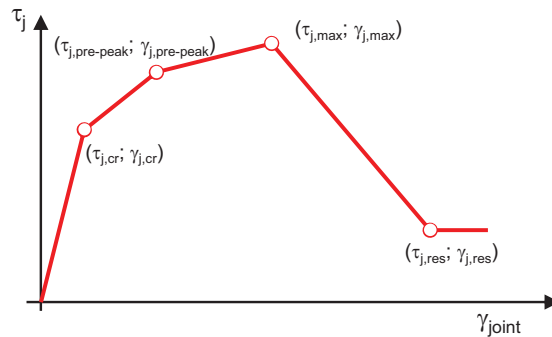
Fig. (4). Main characteristic points of the adopted backbone for the joint panel.

The (τ_j - γ_{joint}) relationship for the joint panel is obtained through the experimentally measured joint shear stress-strain responses, by means of experimental tests conducted on the investigated joint typology that reported these data, namely by means of the (four) tests presented in [20] and the (two) tests by [19]. The experimental joint envelopes for these six tests have been first made symmetric (since specimens were all symmetrically reinforced) by averaging experimental shear stress and strain values between positive and negative loading directions at each drift level. Then, these responses were quadri-linearized, clearly identifying the four required characteristic points introduced before (Fig. **4**).

About the ascending branch of behavior, cracking and peak points of this quadri-linearized response correspond to the first significant change in its slope and to the peak condition, respectively. Moreover, joint stress corresponding to joint cracking can be well predicted by the model proposed by Uzumeri [32], as highlighted in [19, 20]. The pre-peak point is selected to obtain the best-matching with the experimental envelopes for tests in which joint shear failure occurs without the yielding of longitudinal rebars (J-failure); whereas, the pre-peak joint stress can be assumed equal to the joint shear stress corresponding to beam yielding ($\tau_{j,y}$) if joint shear failure occurs after the yielding of longitudinal rebars (BJ-failure).

For each test, it is assumed that the softening branch starts from the peak-load point and goes on up to the joint shear value corresponding to the beam load at the last imposed drift level (residual strength). The corresponding (residual) joint shear strain should be defined. To this end, note that, generally, the experimental response of the joint panel was considered reliable only until the peak load is reached. Therefore, the slope of the softening branch or, equivalently, the joint shear strain corresponding to the end of the softening branch, should be empirically calibrated to reproduce the experimentally observed softening stiffness on the global response. The calibration phase of this key parameter can be extended also to other tests from literature belonging to the collected database and similar to the six tests adopted to calibrate the ascending branch, for which the Authors did not provide any experimental measures about joint shear strains, and with different anchorage details of beam bars, axial load level or buckling slenderness ratio of column rebars passing through the unreinforced joint region. On the whole, ten tests have been considered to investigate about the variability of the softening slope of the joint response due to such parameters, considering tests by Melo *et al*. [12] (TPA2, TPB2, TPC) and Genesio [33] (2D-pre1970s), together with tests presented in [19] and [20]. Basically, first, flexural deformability and fixed-end-rotation contribution are mechanically obtained (according to the monotonic bond strength model by [34]), for each test, as better clarified in Section 6, and then the softening slope of the joint spring is empirically calibrated in order to numerically reproduce the experimental global softening branch of the experimental response (similarly to [35]). This calibration procedure of the softening branch finally provides the softening stiffness shown in Fig. (**5a**), with dotted lines. In particular, in Fig. (**5a**), the six tests adopted to calibrate also the ascending branch of behavior of the joint shear behavior are reported, together with their mean curve (in red); whereas in Fig. (**5b**) such a mean curve is compared with the mean curve of the joint shear behaviour for which the softening slope is evaluated considering all the (ten) analysed tests. The curves reported in Fig. (**5b**) are exactly coincident until peak load is achieved (since the ascending branch is always calibrated on the basis of the tests shown in Fig. (**5a**), whereas, their softening branches are only slightly different. Anyway, the mean joint shear stress-strain relationship (in black in Fig. (**5b**)) is finally adopted in numerical simulations reported in Section 6.

(a)   (b)
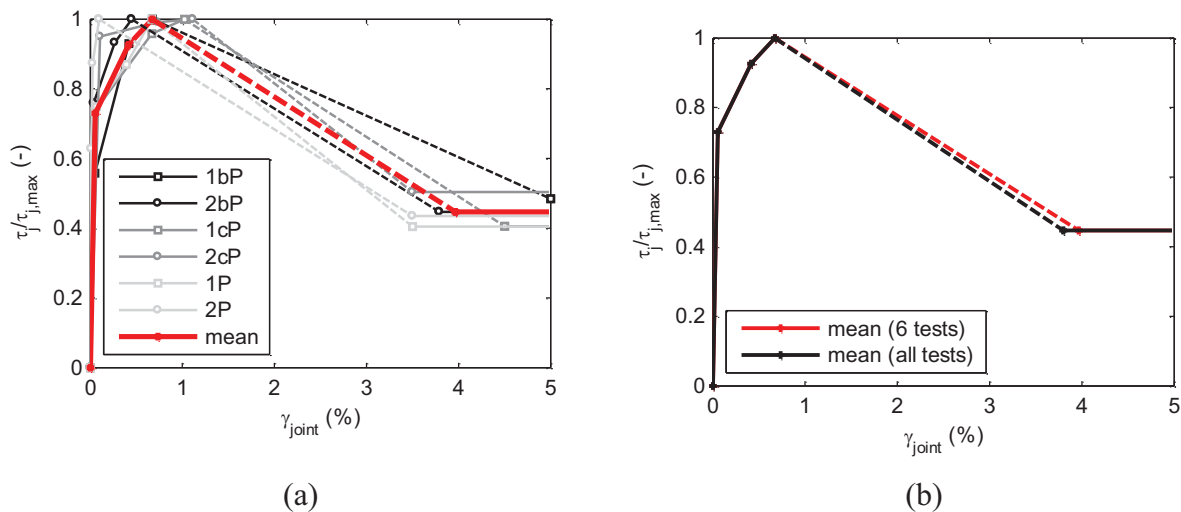
Fig. (5). Quadri-linearized and normalized joint shear behaviour.

Finally, the coordinates of the four obtained characteristic points of the joint panel response are reported in Table **5**.

Table. 5. Joint panel shear behaviour: characteristic points.

Backbone Point	τ_j	γ_{joint}
cracking	Model by Uzumeri [32]	0.05%
pre-peak	$0.93 \cdot \tau_{j,max}$ (if J-failure); $\tau_{j,y}$ (if BJ-failure)	0.42%
peak	Eq. (6)	0.67%
residual	$0.42 \cdot \tau_{j,max}$	3.80%

5. CYCLIC BEHAVIOUR

The same tests adopted for the calibration of the (ascending part of the) backbone described above are used to calibrate the cyclic behaviour of the joint shear stress-strain response. The calibration is performed in OpenSees software [36] on the basis of the hysteresis rules characterizing the *Pinching4* uniaxial material (Fig. **6**). The backbone of this material is defined by four points in negative and in positive directions. *Pinching4* also allows modeling the cyclic degradation of unloading and reloading stiffness (through the parameters *gk* and *gD*, respectively), degradation in strength (through the parameters *gF*) and pinching effects (through the parameters *rDisp, rForce* and *uForce*).
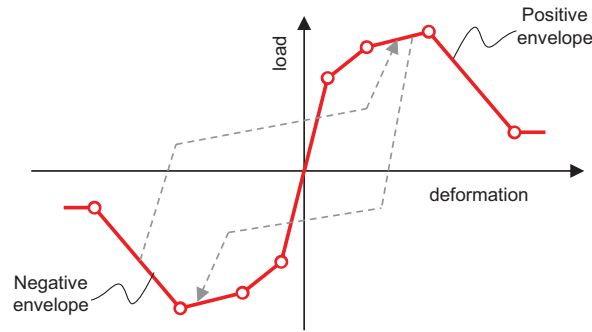
Fig. (6). Pinching4 uniaxial material in OpenSees.

The calibration-phase of these key parameters was performed starting from the experimental shear stress-strain backbones and minimizing the error in terms of dissipated energy between the numerical and the experimental responses. No degradation in strength was introduced (namely all *gF* parameters were set equal to zero) since it is already included in the backbone of the joint response obtained from experimental data. Fig. (**7**) shows the comparison between numerical and experimental cyclic responses in terms of joint shear stress-strain for two of the analysed tests. Finally, Table **6** reports the mean values of the calibrated parameters adopted to fit the experimental response of the analyzed non-ductile exterior beam-column joints.
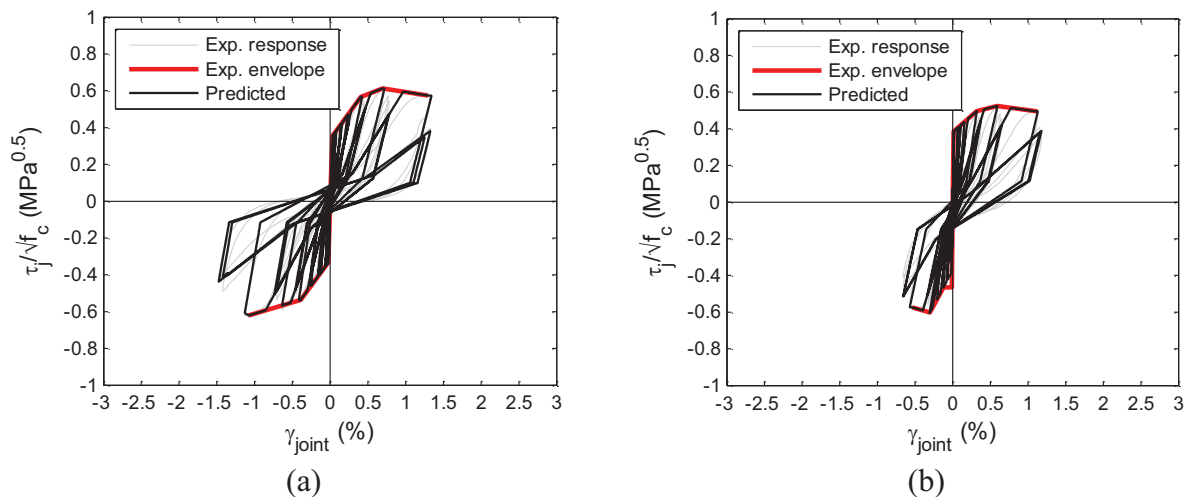

Fig. (7). Examples of results of the calibration for *Pinching 4* hysteretic parameters - Tests #1bP **(a)**, #2bP **(b)** by De Risi and Verderame (2017).

Table. 6. Results of the calibration of joint panel hysteretic behaviour through Pinching 4 material.

Test #	1P	2P	1bP	2bP	1cP	2cP	mean
rDispP	0.2	0.2	0.30	0.30	-0.30	0.30	0.23
rDispN	0.3	0.3	0.30	0.30	0.30	0.30	

(Table 6) contd.....

Test #	1P	2P	1bP	2bP	1cP	2cP	mean
rForceP	0.25	0.25	0.25	0.25	0.05	0.30	0.23
rForceN	0.25	0.25	0.25	0.25	0.25	0.20	
uForceP	-0.2	-0.2	-0.20	-0.20	-0.30	-0.20	-0.21
uForceN	-0.2	-0.2	-0.20	-0.20	-0.20	-0.20	
gK_1	0.75	0.75	0.85	0.85	0.70	0.60	0.75
gK_{lim}	0.96	0.96	0.96	0.96	0.96	0.96	0.96
gD_1	0.4	0.4	0.50	0.50	0.30	0.30	0.40
gD_3	0.3	0.25	0.50	0.50	0	0	0.25
gD_{lim}	0.7	0.7	0.70	0.70	0.70	0.70	0.70
gF_i (i=1,..4)	0	0	0	0	0	0	0
gE	100	100	100	100	100	100	100
$gK_2 = gK_3 = gK_4 = 0$; $gD_2 = gD_4 = 0$; dmgType=cycle							

6. VALIDATION OF THE PROPOSAL

Experimental tests belonging to the collected database have been reproduced through numerical simulations performed in OpenSees platform [36].

The flexural response of beams and columns is modelled in a fiber approach. Concrete and steel properties were obtained from the test programs for each test. In particular, Mander *et al*., model [27] was adopted for concrete, and an elastic-plastic-hardening stress-strain relationship [37] steel model was used for steel (*Concrete04* and *Reinforcing Steel* uniaxial materials in OpenSees, respectively). The response of the beam-column joint is modeled through the adoption of two kinds of rotational springs see Fig. (**8**): the first one is located in the centreline of the joint panel and it represents its shear behaviour; the other ones are located at the interfaces between the joint and the adjacent beam/columns and represent the bond-slip contribution.
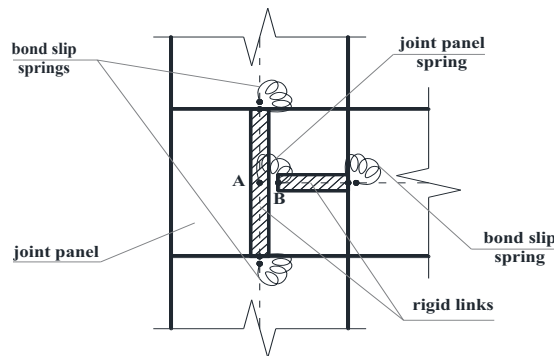

Fig. (8). Numerical model for exterior beam-column joints.

The joint panel zone model is the so-called "scissors" model [38], implemented by defining rigid offsets spreading within the joint region and two nodes (A and B in Fig. (**8**)) overlapped at the center of the joint panel, connected by means of a zero-length rotational spring that allows only relative rotations. The joint panel spring is implemented with a zero-length element defined by a four-point backbone moment-rotation relationship by the adoption of the *Pinching4* uniaxial material in OpenSees. The deformability parameter "rotation" described by this spring coincides with the shear deformation of the joint panel zone (γ_{joint}). Finally, from equilibrium equation, for each characteristic point of the backbone of the joint panel spring (defined in Section 4), the moment transferred through the rotational spring M_j can be calculated as a function of the joint shear stress τ_j, as shown in Eq. (7):

$$M_j = \tau_j A_{jh} \frac{1}{\dfrac{1 - h_c/2L'_b}{d^*} - \dfrac{1}{2L'_c}} \qquad (7)$$

where L'_b and L'_c are the beam and column length, respectively.

The deformability contribution due to the slippage of beam/columns longitudinal rebars anchored into the joint core (fixed-end-rotation) is reproduced through another zero-length element introduced at the beam/columns-joint interfaces.

The related M-Θ_{slip} relationship is calculated in a mechanical approach by using analytical bond-slip models from literature. The procedure described above requires the selection of a proper bond strength model for plain bars and the definition of the ($\tau_{s,h}$ - slip$_h$) relationship related to the end-hook. Unfortunately, a very limited number of studies is available in the literature on bond–slip mechanisms in structural elements with plain bars with respect to deformed bars. Certainly, very low values for the bond strength ($\tau_{b,max}$) are proposed in literature and codes due to the bad quality of the concrete-steel interaction. As a matter of fact, $\tau_{b,max}$=0.15$\sqrt{f_c}$ or $\tau_{b,max}$=0.30$\sqrt{f_c}$ are suggested by CEB-Fib [39] in "poor" and "good" bond conditions, respectively.

Herein, the fixed-end-rotation contribution is reproduced as in De Risi *et al*. [40]. More in details, in order to calculate the M-Θ_s relationship, the cyclic moment-curvature relationship (M-ϕ) is calculated first, under a given imposed cyclic path of curvatures. Then, for each value of ϕ, the slip (s) at the loaded end of the anchored bars is evaluated at the top and bottom layers as a function of the corresponding strain (ε) in the reinforcement. To this end, the finite difference method is applied, discretizing the straight portion (l_d) of the anchored bar in a number of sub-portions of equal length; then, the problem is solved using equilibrium and compatibility equations at each section of the discretized bar, employing the stress-strain constitutive relationship of the reinforcement steel and the bond strength-slip cyclic relationship proposed by [34]. The hook deformability contribution is taken into account by means of the $\tau_{s,h}$-s_h relationship by [41]. Then, the rotation Θ_s corresponding to the calculated slip in the top and bottom reinforcement layers is evaluated as the difference between the two slip values (s_{in}-s_{out}) divided by the distance between the reinforcement layers.

The comparison between experimental responses and numerical simulations based on the assumptions explained above is finally shown in Fig. (**9**) for some of the analyzed tests belonging to the collected database. Note that, in Fig. (**9**), the numerical joint shear strength has been scaled up to the experimental strength (the mean value between positive and negative loading directions), in order to deprive the comparison from the evaluation of predictive capacity of the strength model (issue already analysed in Section 3), and to focus the attention on deformation predictive capacity and hysteretic behaviour. From these comparisons, it can be observed that:

- elastic stiffness is well reproduced;
- global deformability is only slightly underestimated at peak load;
- the numerical responses well reproduce also softening stiffness and residual strength, thanks to the calibration of such parameters (graphically reported in Fig. (**2b**).
- numerical hysteretic responses well predict unloading and reloading stiffness degradation and pinching effect for all the investigated tests.
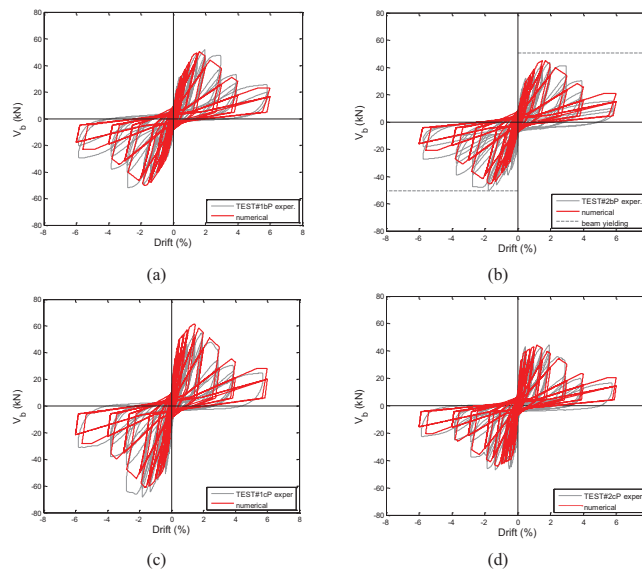

Fig. (9). Experimental versus numerical comparisons.

CONCLUSION

In this work, an empirical macro-modeling approach was proposed for these elements, suitable for extensive nonlinear analyses.

First, a specific homogeneous database of (sixteen) experimental tests about exterior unreinforced joints with hook-ended plain bars in beam and columns was collected and analysed. Based on this dataset, the prediction capacity of the main existing joint strength models from literature was evaluated, thus concluding that: (i) main shear strength models proposed in literature for unreinforced beam-column joints with deformed bars overestimate, on average, the experimental joint shear strength; (ii) the lonely strength model proposed for unreinforced joints with hook-ended plain bars underestimates the experimental results and fails in considering the role of joint aspect ratio and beam longitudinal reinforcement ratio on joint shear strength.

Therefore, a new simple shear model, empirically-based, was proposed herein and validated by means of the experimental data. It was noted that the mean predicted-to-experimental shear strength ratio is equal to 1.00 if all the tests are considered with a quite limited coefficient of variation (19%), thus finally confirming a good accuracy of the proposed model. Together with the joint shear strength assessment, a complete characterization of the nonlinear local response of the joint panel was calibrated on the basis of tests which experimentally measured and provided the joint shear strain evolution. Therefore, the joint panel constitutive parameters were defined to reproduce the experimental joint shear stress-strain behavior, also considering its hysteretic behavior and reproducing it by means of the *Pinching4* uniaxial material in OpenSees platform.

The whole proposal was finally validated by means of numerical-versus-experimental comparisons, proving that: (i) elastic stiffness and global deformability are well reproduced; (ii) the numerical responses also reproduce softening stiffness and residual strength; (iii) numerical hysteretic responses well predict unloading and reloading stiffness degradation and pinching effect for all the investigated tests.

CONSENT FOR PUBLICATION

We obtained the written informed consent from each subject or subject's parent.

CONFLICT OF INTEREST

The authors declare no conflict of interest, financial or otherwise.

ACKNOWLEDGEMENTS

REFERENCES

[1]   J.P. Moehle, and S.A. Mahin, Observations on the behavior of reinforced concrete buildings during earthquakes Earthquake-Resistant Concrete Structures Inelastic Response and Design SP-127, ACI, ed. S.K. Ghosh, Detroit,1991.

[2]   P. Ricci, F. De Luca, and G.M. Verderame, "6th April 2009 L'aquila earthquake, italy: Reinforced concrete building performance", *Bull. Earthquake Eng.,* vol. 9, no. 1, pp. 285-305, 2011.
[http://dx.doi.org/10.1007/s10518-010-9204-8]

[3]   C. Menna, R. Frascadore, C. Moroni, G.P. Lignola, G. De Martino, A. Salzano, M. Di Ludovico, A. Prota, G. Manfredi, and E. Cosenza, Rapporto fotografico relativo ai danni subiti da alcuni edifici a seguito del sisma del centro Italia del, 2016.

[4]   O.C. Celik, and B.R. Ellingwood, "Modeling beam-column joints in fragility assessment of gravity load designed reinforced concrete frames", *J. Earthquake Eng.,* vol. 12, pp. 357-381, 2008.
[http://dx.doi.org/10.1080/13632460701457215]

[5]   S. Park, and K.M. Mosalam, "Simulation of reinforced concrete frames with non-ductile beam-column joints", *Earthq. Spectra,* vol. 29, no. 1, pp. 233-257, 2013.
[http://dx.doi.org/10.1193/1.4000100]

[6]   C. Clyde, C.P. Pantelides, and L.D. Reaveley, Reaveley, Performance-based evaluation of exterior reinforced concrete buildings joints for seismic excitation. *PEER Report, No. 2000/05.*, Pacific Earthquake Engineering Research Center, University of California: Berkeley, USA, 2000.

[7]   C.P. Pantelides, J. Hansen, J. Nadauld, and L.D. Reaveley, Assessment of reinforced concrete building exterior joints with substandard details. *PEER Report, No. 2002/18.*, Pacific Earthquake Engineering Research Center, University of California: Berkeley, USA, 2002.

[8]   A. Masi, G. Santarsiero, and D. Nigro, "Cyclic tests on external RC beam-column joints: Role of seismic design level and axial load value on the ultimate capacity", *J. Earth. Eng,* vol. 17, no. 1, pp. 110-136, 2013.

[9]   A. Liu, *"Seismic assessment and retrofit of pre-1970s reinforced concrete frame structures"*, PhD Thesis, University of Canterbury: New Zeland, 2001.

[10]   T. H. Chen, *"Retrofit strategy of non-seismically designed frame systems based on a metallic haunch system"*, Thesis, University of canterbury, New Zeland, 2006.

[11]   I. Bedirhanoglu, A. Ilki, S. Pujol, and N. Kumbasar, "Behavior of deficient joints with plain bars and low-strength concrete", *ACI Struct. J.,* vol. 107, no. 03, p. 300, 2010.

[12]   J. Melo, H. Varum, T. Rossetto, and A. Costa, "Cyclic response of RC beam-column joints reinforced with plain bars: An experimental testing campaign", In: *Proceedings of the 15th World Conference on Earthquake Engineering.*Lisbon, Portugal pp. 24-28, 2012

[13]   S. Pampanin, G.M. Calvi, and M. Moratti, "Seismic behavior of RC beam-column joints designed for gravity only", *In: 12th European Conference on Earthquake Engineering* London, United Kingdom, 2002.

[14]   C. Fernandes, J. Melo, H. Varum, and A. Costa, "Cyclic behavior of substandard reinforced concrete beam-column joints with plain bars", *ACI Struct. J.,* vol. 110, no. 1, p. 137, 2013.

[15]   F. Braga, R. Gigliotti, and M. Laterza, "R/C existing structures with smooth reinforcing bars: Experimental behaviour of beam-column joints subject to cyclic lateral loads", *Open Constr. Build. Technol. J.,* vol. 3, pp. 52-67, 2009.
        [http://dx.doi.org/10.2174/1874836800903010052]

[16]   C. Beschi, P. Riva, G. Metelli, and A. Meda, "HPFRC jacketing of non-seismically detailed RC corner joints", *J. Earthquake Eng.,* vol. 19, no. 1, pp. 25-47, 2015.
        [http://dx.doi.org/10.1080/13632469.2014.948646]

[17]   C. Fernandes, H. Varum, and A. Costa, "Importance of the bond-slip mechanism in the numerical simulation of the cyclic response of RC elements with plain reinforcing bars", *Eng. Struct.,* vol. 56, pp. 396-406, 2013.
        [http://dx.doi.org/10.1016/j.engstruct.2013.05.013]

[18]   M. T. De Risi, P. Ricci, G.M. Verderame, and G. Manfredi, "Experimental assessment of unreinforced exterior beam-column joints with deformed bars", *Eng. Struct.,* vol. 112, pp. 215-232, 2016.

[19]   P. Ricci, M.T. De Risi, G.M. Verderame, and G. Manfredi, "Experimental tests of unreinforced exterior beam-column joints with plain bars", *Eng. Struct.,* vol. 118, pp. 178-194, 2016.
        [http://dx.doi.org/10.1016/j.engstruct.2016.03.033]

[20]   M.T. De Risi, and G.M. Verderame, "Experimental assessment and numerical modelling of exterior non-conforming beam-column joints with plain bars", *Eng. Struct.,* vol. 150, pp. 115-134, 2017.
        [http://dx.doi.org/10.1016/j.engstruct.2017.07.039]

[21]   G.M. Verderame, M.T. De Risi, and P. Ricci, "Experimental investigation of unreinforced exterior beam-column joints with plain and deformed bars", *J. Earthq. Eng.,* vol. 22, no. 3, p. 2018, 2018.

[22]   M.J.N. Priestley, *Myths and fallacies in earthquake engineering, revisited.*. The Mallet Milne Lecture. IUSS Press: Pavia, Italy, 2003

[23]   S. Park, and K.M. Mosalam, "Analytical model for predicting the shear strength of unreinforced exterior beam-column joints", *ACI Struct. J.,* vol. 109, pp. 149-159, 2012.

[24]   G. Metelli, F. Messali, C. Beschi, and P. Riva, "A model for beam–column corner joints of existing RC frame subjected to cyclic loading", *Eng. Struct.,* vol. 89, pp. 79-92, 2015.
        [http://dx.doi.org/10.1016/j.engstruct.2015.01.038]

[25]   S.J. Hwang, and H.J. Lee, "Analytical model for predicting shear strengths of exterior reinforced concrete beam-column joints for seismic resistance", *ACI Struct. J.,* vol. 96, no. 5, pp. 846-858, 1999.

[26]   U. Akguzel, and S. Pampanin, "Effects of variation of axial load and bidirectional loading on seismic performance of GFRP retrofitted reinforced concrete exterior beam-column joints", *J. Compos. Constr.,* vol. 14, no. 1, pp. 94-104, 2010.
        [http://dx.doi.org/10.1061/(ASCE)1090-0268(2010)14:1(94)]

[27]   J.B. Mander, M.J.N. Priestley, and R. Park, "Theoretical stress-strain model for confined concrete", *ASCE, Struct. Engi. J.,* vol. 114, no. 8, pp. 1804-1826, 1988.
        [http://dx.doi.org/10.1061/(ASCE)0733-9445(1988)114:8(1804)]

[28]   M.J.N. Priestley, "Displacement-based seismic assessment of reinforced concrete buildings", *J. Earthquake Eng.,* vol. 1, pp. 157-192, 1997.
        [http://dx.doi.org/10.1080/13632469708962365]

[29]   M.J.N. Priestley, ASCE/SEI 41, "Seismic rehabilitation of existing buildings". American Society of Civil Engineers: Reston, VA, USA, 2007.

[30]   J.S. Jeon, A. Shafieezadeh, and R. DesRoches, "Statistical models for shear strength of RC beam-column joints using machine-learning techniques", *Earthquake Eng. Struct. Dynam.,* vol. 43, no. 14, pp. 2075-2095, 2014.
        [http://dx.doi.org/10.1002/eqe.2437]

[31] M.T. De Risi, P. Ricci, and G.M. Verderame, "Modelling exterior unreinforced beam-column joints in seismic analysis of non-ductile RC frames", *Earthquake Eng. Struct. Dynam.,* vol. 46, no. 6, pp. 899-923, 2017.
      [http://dx.doi.org/10.1002/eqe.2835]

[32] S.M. Uzumeri, "Strength and ductility of cast-in-place beam-column joints", In: *From the American concrete institute annual convention, symposium on reinforced concrete structures in seismic zones*. San Francisco, No. SP-53, 1977.

[33] G. Genesio, *"Seismic assessment of RC exterior beam-column joints and retrofit with haunches using post-installed anchors"*, Ph.D. Thesis, University of Stuttgart, Germany, 2012.

[34] G.M. Verderame, G. De Carlo, P. Ricci, and G. Fabbrocino, "Cyclic bond behaviour of plain bars. Part II: Analytical investigation", *Constr. Build. Mater.,* vol. 23, no. 2009, pp. 3512-3522, 2009.

[35] J.S. Jeon, L.N. Lowes, R. DesRoches, and I. Brilakis, "Fragility curves for non-ductile reinforced concrete frames that exhibit different component response mechanisms", *Eng. Struct.,* vol. 85, pp. 127-143, 2015.
      [http://dx.doi.org/10.1016/j.engstruct.2014.12.009]

[36] F. McKenna, G.L. Fenves, and M.H. Scott, "OpenSees: Open System for Earthquake Engineering Simulation", Pacific Earthquake Engineering Research Center. University of California: Berkeley, CA, USA, [Online] Available on http://opensees.berkeley.edu, 2010, 2017

[37] G.A. Chang, and J.B. Mander, *Seismic energy based fatigue damage analysis of bridge columns: Part I-Evaluation of seismic capacity.,* National Center for Earthquake Engineering Research: Buffalo, NY, 1994, p. 222.

[38] S. Alath, and S.K. Kunnath, "Modelling inelastic shear deformations in RC beam–column joints", In: *Engineering mechanics proceedings of 10th conference*. May 21-24, University of Colorado: Boulder, Colorado, vol. 2. New York: ASCE: pp. 822–825, 1995.

[39] C.E.B. Fib, Model Code - first complete draft". Fédération Internationale du Béton fib/International Federation for Structural Concrete, 2010.

[40] M.T. De Resi, P Ricci, and GM Verderame, "Cyclic response and nonlinear modeling of exterior unreinforced RC beam-column joints with plain longitudinal bars", In: *COMPDYN 2017-6th ECCOMAS Thematic Conference on Computational Methods in Structural Dynamics and Earthquake Engineering*. 15-17 June. Rhodes Island, Greece, 2017.

[41] G. Fabbrocino, G.M. Verderame, and G. Manfredi, "Experimental behaviour of anchored smooth rebars in old type reinforced concrete buildings", *Eng. Struct.,* vol. 27, no. 10, pp. 1575-1585, 2005.
      [http://dx.doi.org/10.1016/j.engstruct.2005.05.002]

[42] M. Moratti, Risposta sismica di nodi-trave colonna progettati per soli carichi di gravità: studi analitici e sperimentali, 2012.